Microchim Acta (2016) 183:1449–1458
DOI 10.1007/s00604-016-1780-0

ORIGINAL PAPER

Air-assisted dispersive micro-solid phase extraction of polycyclic aromatic hydrocarbons using a magnetic graphitic carbon nitride nanocomposite

Maryam Rajabi[1] · **Ahmad Ghoochani Moghadam**[1] · **Behruz Barfi**[1] · **Alireza Asghari**[1]

Received: 13 November 2015 / Accepted: 3 February 2016 / Published online: 12 February 2016

Abstract An air-assisted dispersive micro solid phase extraction method (AA-dμ-SPE) is described that is based on the use of a magnetic graphitic carbon nitride (g-C_3N_4/Fe_3O_4) nanocomposite. In AA-dμ-SPE, magnetic nanocomposite was dispersed into the aqueous sample solution by air bubbles, which promoted the analytes adsorption. The magnetic adsorbents were then separated from sample solution using a magnetic field. The method was shown to be efficient, rapid and reliable to extract the polycyclic aromatic hydrocarbons (PAHs) from biological samples prior to their determination by GC with FID detection. The nanocomposite was characterized by X-ray diffraction, FT-IR spectroscopy, scanning electron microscopy, transmission electron microscopy, vibrating sample magnetometer and thermogravimetric techniques. A main reason of selection of the g-C_3N_4/Fe_3O_4 nanocomposites as adsorbent is their high affinities to PAHs and ease of collection from the solution. Several parameters affecting adsorption and desorption phenomena were studied. Under optimum conditions, the limits of detection, linear ranges and relative standard deviations (RSDs, for $n = 6$) were ranged from 0.3 to 0.6 (ng mL^{-1}), 1 to 100 ng mL^{-1}, and 3.49 to 5.94 %. The adsorbents can be reused up to 7 times. The method was applied for the determination of naphthalene, fluorene, phenanthrene, anthracene and pyrene in (spiked) saliva and blood samples, and satisfactory results were achieved.

Keywords Air-assisted dispersive microextraction · Magnetic extraction · Magnetic nanoparticles · Nanomaterial · Melamine · GC–FID · FTIR · Thermogravimetric analysis

Introduction

Polycyclic aromatic hydrocarbons (PAHs) are produced as byproducts during fuel burning or carbon-containing organic substances and found in oil, coal and tar deposit [1]. Natural emissions including volcano eruptions and forest fires can also emit these compounds [2]. Due to their mutagenic, carcinogenic, and endocrine-disrupting properties, these compounds are included in the European Union (EU) and United States Environmental Protection Agency (USEPA) priority pollutant list [3]. In this way, identification and determination of PAHs in environmental samples is an important topic because of their adverse effects on humans and on soil organisms and plants, even at low concentrations of these compounds. However, in most cases, the amounts of PAHs are below detection limit of many analytical techniques, and matrix interferences come along with their determination. Hence, preliminary separation and pre-concentration of these compounds is usually required.

Current methods for the sample preparation and pre-concentration, in terms of extractant phase can be subdivided into solid phase based extraction [4–6], liquid phase based microextraction [7, 8] and solid-phase based microextraction [9, 10].

The most preferred method for sample preparation and pre-concentration of PAHs is solid-phase extraction (SPE) [11, 12] because of its high enrichment, simplicity, reduction of sample matrix effects and high recovery [13]. The bottleneck of SPE is the sample loading

Electronic supplementary material The online version of this article (doi:10.1007/s00604-016-1780-0) contains supplementary material, which is available to authorized users.

✉ Maryam Rajabi
mrajabi@semnan.ac.ir; marajabi@gmail.com

[1] Department of Chemistry, Semnan University, Semnan 35195-363, Iran

step, which can be performed by gravity flow or pressure/vacuum-assisted. Depending on the instrumental limit of detection, and therefore, on the amount of sample to be extracted, sample loading can require a relatively long period of time. Besides, in most cases, the aggregation tendency of solid particles reduces the active area that limits the full exploitation of the potential extractability.

Dispersive solid phase extraction (D-SPE) is a modified version of SPE that considerably reduces the time consumed, and simplifies the extraction process. In this method, extraction is not carried out in a cartridge, column or disk but in the bulk solution, which leads to more rapidity and ease of operation compared with the conventional SPE. The method consists of two critical steps: i) dispersion, and ii) phase separation. The second step is usually performed by centrifugation, which is very effective. However, it makes the overall procedure time-consuming. In this sense, development of a D-SPE method which could avoid the use of centrifugation is of great importance.

Nanoscale carbon-based materials, such as graphene (G) [14, 15], graphene oxide (GO) [16, 17] and carbon nanotubes (CNTs) are used as solid sorbent materials due to their ultrahigh surface area and high chemical stability. g-C_3N_4 sheets consist of a hexagonal ring-based carbon-nitrogen network, and they have a strong affinity for aromatic compounds based on large delocalized π-electron structure [14]. g-C_3N_4 has received vast interest and was applied in various fields, such as photocatalysis [18], hydrogen storage [19], lithium-ion battery [20], electrogenerated chemiluminescence [21] and fluorescent sensor. Notably, g-C_3N_4 can be used as a novel sorbent for SPE method.

Magnetic nanoparticles (MNPs) have attracted much attention in preconcentration of target analytes from different real samples, due to their gentle separation and non-destructive effects on biological analytes. As a main advantage, target analytes captured to them can be easily and selectively removed from the sample with an external magnet [22]. After washing out the contaminants, the isolated target compounds can be eluted and used for further analysis [23]. In this way, simple collection of the magnetic materials and chemical affinity of PAHs are combined. This results in the facile, fast and efficient preconcentration of the interested analytes. As a consequence, the g-C_3N_4/Fe_3O_4 nanocomposites may be favorably used as sorbents for preconcentration of PAHs.

In the present study, an air-assisted dispersive micro-solid phase extraction method (AA-dμ-SPE) (based on using magnetic graphitic carbon nitride nanocomposites as an adsorbents) is presented to extract the PAHs with a low level consumption of adsorbent and without using a toxic organic solvent. A few micrograms of the g-C_3N_4/Fe_3O_4 nanocomposites were transferred into aqueous sample solution in a glass vial, and then the mixture was repeatedly sucked into a glass syringe and then injected into the glass vial. By this action, the interaction between magnetic adsorbent and analytes increased more and more [24]. After performing predetermined cycles, the magnetic adsorbents were separated from water by a magnetic field. The adsorbed analytes were eluted with ethanol/acetone and 1 μL of the solution was injected into a gas chromatography with flame ionization detection (GC–FID) system for further analysis. Effective parameters such as amount of sorbent, number of extraction cycles, pH value, ionic strength, type and volume of eluting solvent were investigated to achieve the best conditions for extraction of the analytes from bio-fluid and water samples.

Experimental

Reagents and solvents

All chemicals used were of analytical grade. The PAHs standard, including naphthalene (Naph), fluorene (Fl), phenanthrene (Phen), anthracene (An), pyrene (Pyr), were purchased from Fluka (Buchs, Switzerland). Biphenyl (as internal standard) was purchased from Sigma (Steinheim, Germany). Solvents including methanol, ethanol, acetone, acetonitrile, ammonia and hydrochloric acid (HCl, 36 %) were obtained from Merck (Darmstadt, Germany). Sodium chloride, ferric chloride ($FeCl_3 \cdot 6H_2O$), ferrous chloride ($FeCl_2 \cdot 4H_2O$) and melamine were also obtained from Merck.

Standard stock solutions of five PAHs were prepared at 1000 μg mL^{-1} level in methanol for each compound. All solutions were stored in the dark at 4 °C. All working solutions were prepared by appropriately diluting the stock standard solution with ultra-pure water.

Instrumentation

Separation and detection of the analytes were performed by a gas chromatograph (GC-17 A, Shimadzu, Japan) equipped with a splitless/split injector and a flame ionization detector. Helium (purity 99.999 %) was used as the carrier gas at the constant flow rate of 4 mL min^{-1}. The temperatures of injector and detector were set at 280 °C and 320 °C, respectively. The injection port was operated at splitless mode and with sampling time 1 min. For FID, hydrogen gas was generated with a hydrogen generator (OPGU-2200S, Shimadzu, Japan). A 30 m BP-10 SGE fused-silica capillary column (0.32 mm i.d. and 0.25 μm film thickness) was applied for separation of PAHs. Oven temperature program was: started from 50 °C, held for 1 min, increased to 190 °C at 30 °C min^{-1}, held for 0 min, increased to 240 °C at 10 °C min^{-1} and then held for 3 min. A 10.0 μL ITO (Fuji, Japan) micro-syringe applied for the collection of sedimented organic solvent and injection into the GC.

A ultrasonic bath (SW3, Switzerland), was employed at a frequency of 50/60 kHz for speed up desorption of PAHs on the sorbents. The phase identification of g-C_3N_4/Fe_3O_4 nanocomposite power was obtained by X-ray diffraction (XRD) on a D8 Bruker XRD (USA) with Cu Kα radiation (35 kV, 15 mA, λ = 1.54051°A). Fourier transform infrared spectroscopy (FT-IR) spectra were recorded on a Shimadzu 8400 s (Japan) spectrophotometer. Thermogravimetric analysis (TGA) of g-C_3N_4/Fe_3O_4 was performed on a LINSEIS TG/DTA (STA PT 1600, Germany) thermogravimetric analyzer, the morphology of g-C_3N_4 and g-C_3N_4/Fe_3O_4 nanocomposite was observed an XL30 Philips (USA) scanning electron microscope.

Synthesis of g-C_3N_4/Fe_3O_4 nanocomposites

The g-C_3N_4 was synthesized by pyrolysis of melamine according to a reported procedure [25]. Typically, 20 g of melamine was put into an alumina crucible with a cover and heated at 550 °C for 4 h in muffle furnace with a ramp rate of 2.5 °C min^{-1}. The obtained yellow product was the g-C_3N_4, and then the bulk g-C_3N_4 was ground to powder. The g-C_3N_4 / Fe_3O_4 nanocomposites were prepared by an in situ precipitation method [26]. In a typical procedure, g-C_3N_4 (125 mg) was dispersed in 500 mL of ethanol/water (1:2) and ultrasonicated for 5 h at room temperature. $FeCl_3 \cdot 6H_2O$ (1.838 g) and $FeCl_2 \cdot 4H_2O$ (0.703 g) were dissolved separately in 20 mL of double-distilled water and added to the suspension of g-C_3N_4. The mixture was stirred at 80 °C for 30 min, and then 10 mL of ammonia solution (NH_4OH) was quickly injected into the reaction mixture. The resulting mixture was stirred for another 30 min, after which the reaction mixture was cooled and washed several times with double-distilled water and absolute alcohol. Finally, obtained precipitate was dried in air at 80 °C for further characterization (Fig. 1).

Extraction procedure

g-C_3N_4/Fe_3O_4 (15 mg) as a adsorbent, 5 g NaCl and 100 mL of the analytes standard mixture solution (0.1 μg mL^{-1} of each analyte) were placed into a glass vial and solution pH adjusted (pH = 7) with 0.1 M HCl and 0.1 M NaOH. By using a glass syringe (10 mL), solution was repeatedly sucked and injected into the glass vial. By this action the interaction between adsorbent and analytes increased more and more. After performing 30 cycles, the adsorbent was separated from solution by a magnetic field during 2 min. 1 mL ethanol/acetone was added to the adsorbent and the glass vial was subsequently subjected to ultrasonic irradiation for 5 min to speed up desorption of the analytes. Afterwards, 1 μL of the collected eluent was injected into a GC for further analysis. The results were reported based on relative response that is defined as proportion of analyte peak area to peak area of internal standard (biphenyl). Figure 2 shows the schematic representation of AA-dμ-SPE.

Sample preparation

Saliva samples were collected from smoker volunteers (aged between 25 to 35 years) in our laboratory. Two types of saliva samples were prepared from a healthy volunteer in our lab: i) blank saliva samples (analytes-free) and ii) model saliva samples. Blank saliva samples were prepared from the smoker volunteers that not smoked cigarettes at least for 1 week, whereas model saliva samples were prepared from the smoker volunteers 30 min after smoking (addicted to smoking cigarettes, at least for 1 month).

An aliquot of 10.0 mL saliva sample was directly transferred to a volumetric flask and diluted to 100.0 mL. Then, the extraction was performed with the AA-dμ-SPE method.

Blood samples were collected from smoker volunteers into Pyrex centrifuge tubes. The tubes were stored on ice for a maximum of 15 min before centrifugation. Blood samples were centrifuged at 10,000 rpm. After separation of plasma in the collection tube with centrifuge, 2.0 mL of upper phase was immediately transferred to a volumetric flask, diluted to 100.0 mL and the extraction performed with the AA-dμ-SPE method.

Results and discussion

The method is based on the withdrawing and pushing out a mixture of sample solution and adsorbent in a glass tube using a single syringe. This simple action leads to efficient dispersion of adsorbent in the sample solution. Collection of the

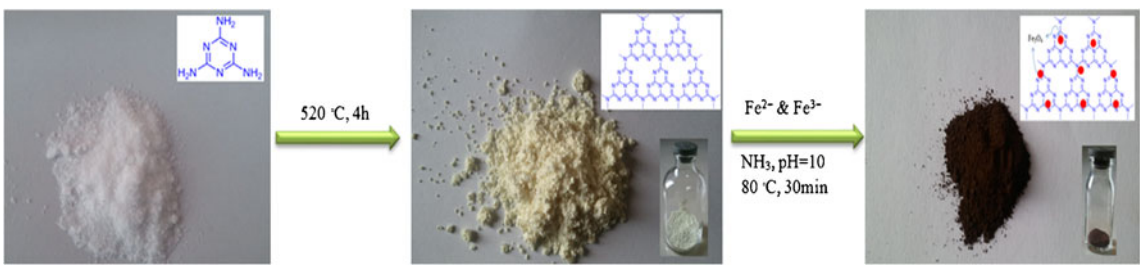

Fig. 1 The photographic pictures of depositing Fe_3O_4 nanoparticles on a g-C_3N_4

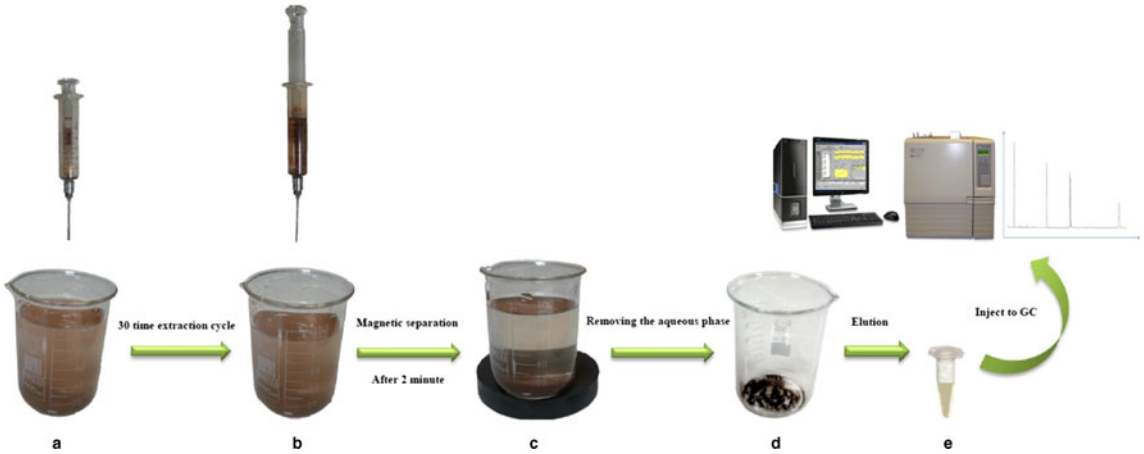

Fig. 2 Schematic representation of AA-dμ-SPE. **a** 100 mL sample solution and 15 mg of adsorbents. **b** Suction and injection of solution using glass syringe was caused to increase of interaction between adsorbents and analytes **c** Adsorbents were separated from water by a magnetic field **d** Aqueous phase removed easily from glass vial **e** Adsorbed analytes eluted and then injected to GC

adsorbent through the extraction (adsorption and desorption steps), was easily performed using a magnet. At the end, the best conditions were selected based on the highest peak areas (or recoveries).

Choice of materials

g-C_3N_4 has a stacked two-dimensional structure (2D sheets of tri-s-triazine connected via tertiary amines) and is made from simple precursors under ambient conditions with a low cost. However, dispersity of g-C_3N_4 in water is much better than graphene (G). These properties suggest the possibility of g-C_3N_4 as a new sorbent for AA-dμ-SPE for the extraction and preconcentration of polycyclic aromatic hydrocarbons. On the other hand, for the simple collection of nanomaterials, immobilizing Fe_3O_4 particles on the surface of nanomaterials is an effective solution, as it can be easily separated from solution with an external magnet.

Characterization of g-C_3N_4/Fe_3O_4

The XRD patterns of the samples are shown in Fig. 1S. The XRD peaks of g-C_3N_4 and Fe_3O_4 were observed in the XRD pattern of the synthesized g-C_3N_4/Fe_3O_4. Diffraction peaks of Fe_3O_4 appeared at the Bragg angles of about 30.02°, 35.61°, 36.20°, 43.28°, 53.16°, 57.18°, 62.78° and 73.57° are respectively ascribed to the (220), (311), (222), (400), (422), (511), (440) and (533) that were in good agreement with the standard magnetite Fe_3O_4. The XRD pattern of the synthesized g-C_3N_4 shows two broad peaks at 2θ = 13.2 ° and 27.3 °. It is well known that g-C_3N_4 is based on tri-s triazine building blocks. The strongest peak at 27.3 ° is close to the peak position of graphite (002), and is due to the interlayer stacking of aromatic systems. The small angle peak at 13.2° is associated with interlayer stacking [27].

Figure 2S shows the FT-IR spectra of pure g-C_3N_4 and the g-C_3N_4/Fe_3O_4 nanocomposites that confirmed the successful formation of g-C_3N_4/Fe_3O_4. The broad Fe-O band in the region from 550 to 650 cm^{-1} is clearly visible at all compositions [26]. The strong absorption peaks can be observed in the range of 1200–1600 cm^{-1}, which corresponded to the stretching mode of C = N bonds. The broad peaks in the range of 3000–3700 cm^{-1} were attributed to the adsorbed H_2O molecules and NH stretching vibration. Additionally, the absorption peak at 810 cm^{-1} was assigned to the characteristic breathing mode of the triazine units [25]. The results indicate that the aromatic g-C_3N_4 owns specific structure leading to its unique absorption ability.

The SEM and TEM images, as shown in Fig. 3, exhibited that Fe_3O_4 nanoparticles were successfully deposited on the surface of the g-C_3N_4 sheets. The surface morphology of the synthesized g-C_3N_4 is seemed to be smooth, after in situ deposition of Fe_3O_4 nanoparticles onto the surface of the g-C_3N_4 (Fig 3c and d). The TEM images (Fig 3e and f) were obvious showed that the distribution of Fe_3O_4 on the surface of g-C_3N_4 is uniform and prevented the agglomeration of Fe_3O_4 nanoparticles. Also, no free Fe_3O_4 nanoparticles were found outside of the g-C_3N_4 sheet. According to the Fig. 3, the particle size of g-C_3N_4 and Fe_3O_4 are 70–180 and 8–12 nm, respectively.

TGA curve of g-C_3N_4/Fe_3O_4 was shown in Fig. 3S. TGA analysis was used to determine the thermal stability of the g-C_3N_4/Fe_3O_4 nanocomposite. The g-C_3N_4/Fe_3O_4 began to decompose when the temperature was over 500 °C, and the total decomposition occurred at the temperature of 690 °C.

The porosity and effective surface area measurements for the g-C_3N_4/Fe_3O_4 nanocomposites were performed by the N_2 equilibrium adsorption isotherms at 77 K (Table 1). The BET surface area of the adsorbent used was 137.713 m^2g^{-1}, with a pore volume of 0.388 cm^3g^{-1}. Also the average pore diameter was found to be 2.371 nm, indicating an appreciable narrow micro-porosity for the g-C_3N_4/Fe_3O_4 nanocomposites.

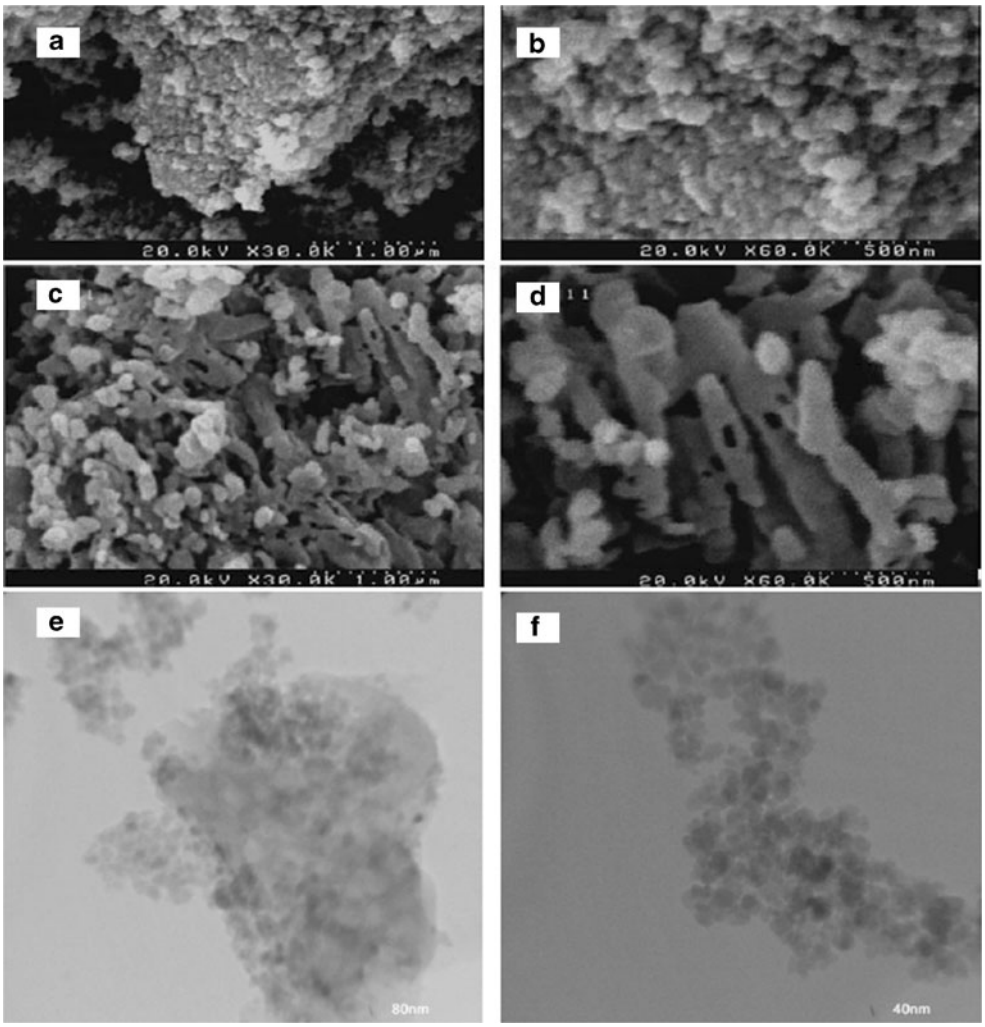

Fig. 3 SEM images (pure g-C_3N_4 (**a**, **b**) and g-C_3N_4/Fe_3O_4 (**c**, **d**)) and TEM images (g-C_3N_4/Fe_3O_4 **e**, **f**)

Magnetic properties of the g-C_3N_4/Fe_3O_4 nanocomposite

To collect and reuse the adsorbent in this study, its preparation with good super-paramagnetism is essential. The magnetic properties of g-C_3N_4/Fe_3O_4 nanocomposites were characterized by a vibrating sample magnetometer (VSM) at room temperature and saturation magnetization value is 44.49 emu g^{-1}. The magnetization curve of g-C_3N_4/Fe_3O_4 nanocomposites is shown in Fig. 4S. This nanocomposite has been successfully applied as a magnetic adsorbent in air-assisted dispersive micro solid phase extraction method.

Table 1 Surface area and porosity of g-C_3N_4/Fe_3O_4 nanocomposites

S_{BET} (m^2 g^{-1})	S_{LAN} (m^2 g^{-1})	V_p (cm^3 g^{-1})	D_p (nm)
137.713	203.333	0.388	2.371

$\boldsymbol{S_{BET}}$: BET surface area; $\boldsymbol{S_{LAN}}$: langmuir surface area; $\boldsymbol{V_p}$: total pore volume; $\boldsymbol{D_p}$: average pore diameter

Optimization of air-assisted dispersive micro-solid phase extraction conditions

In order to evaluate the application ability of the g-C_3N_4/Fe_3O_4 nanocomposites in extraction of PAHs in bio-fluid and water samples, the effective parameters on the adsorption and desorption should be investigated and optimized. A 0.1 μg mL^{-1} of solution mixture was used in the optimization of variables. Effective parameters on the adsorption of PAHs on the g-C_3N_4/Fe_3O_4 surfaces such as amount of adsorbent, number of extraction cycles, ionic strength, pH, and desorption such as type and volume of elution solvent were studied. To achieve the optimum extraction conditions, one-at-a-time (univariate) optimization strategy was used.

Amount of adsorbent

Varying amounts of g-C_3N_4/Fe_3O_4 in the range of 5.0–30.0 mg were evaluated by extracting 100 mL of sample solution, the result being shown in Fig. 5S As it can be observed, by increasing adsorbent amount, analytical signals increase till

15.0 mg and then remain constant. Hence, 15.0 mg of g-C_3N_4/Fe_3O_4 was selected for the further studies.

Number of extraction cycles

In this work, the sample solution was rapidly sucked into a 10 mL glass syringe and then was injected into the tube. The numbers of suction/injection cycles are considered as number of extraction cycles. To reach equilibrium status, numbers of extraction was studied in the range of 5–40 times. The results obtained in Fig. 6S show that by increasing extraction numbers, analytical signals also increase till 30th extraction and then remain constant. Hence, 30 times of extraction was selected for the further studies. It is noted that this step was performed in less than two minute.

Effect of ionic strength

To evaluate effect of the ionic strength in this study, efficiency of extraction from aqueous solution containing 0.1 μg mL^{-1} of each target analyte was investigated in presence of different amounts of sodium chloride (0–10 %, *w*/*v*). Generally, salt addition can decrease the solubility of analytes in the aqueous phase (salting-out effect), thereby improving the extraction efficiency. However, with the increase of ionic strength, the viscosity of the solution increases and the efficiency of the mass transfer process subsequently decrease due to the viscous resistance effect. The results in Fig. 7S indicate, recovery of the analytes increased up to 5 % (*w*/*v*) sodium chloride and after that remained nearly constant in the range of 5–10 % (*w*/*v*) sodium chloride. Finally, 5 % *w*/*v* sodium chloride was chosen as a suitable concentration.

Effect of pH

The pH value of the sample also affects extraction efficiency. The effect of sample pH on the extraction efficiency of analytes was investigated in the range of 3 to12 (Fig. 8S) with the adjustment with HCl or NaOH. Although PAHs exist as neutral molecules under ordinary conditions and are unlikely to be influenced by a change in the solution pH, the pH of the solution may affect the g-C_3N_4/Fe_3O_4 formation and dispersity in water. The results indicated that with decreasing in pH, the analytes recoveries were decreased in the pH range of 3–7. Acidic conditions may cause some leaching of Fe_3O_4, thereby decreasing the adsorption of PAHs on the g-C_3N_4/Fe_3O_4 nanocomposite. In the pH range of 7–12, recovery remained nearly constant. Hence, pH = 7 was selected for the further studies.

Type of solvent elution

Selecting a suitable elution solvent is critical in the AA-dμ-SPE process to achieve high analytical signal and extraction efficiency depending on the properties of eluent. In order to find the suitable elution solvent, four organic solvents and mixture including, acetonitrile, acetone, methanol and ethanol/acetone were compared for their eluting efficiency. As shown in Fig. 9S, desorption efficiency was significantly affected by the eluent and ethanol/acetone resulted the highest elution efficiency for the target analytes. Therefore, ethanol/acetone was selected as an optimum solvent elution.

Volume of elution solvent

To examine effect of volume of elution solvent, experiments involving different volumes of elution solvent (0.75, 1.0, 1.5, and 2.0 mL) were studied. Fig. 10S shows the influence of volume of elution solvent on the analytes extraction. It can be observed that recovery of analytes increased with increasing volume of elution solvent up to 1.0 mL and then decreased. In lower elution solvent volumes, elution of analytes are not completed. High recoveries along with good repeatability were obtained when 1.0 mL of elution solvent was used. Therefore, 1.0 mL was selected as the optimum volume of the elution solvent in this study. The best experimental conditions were found to be as: amount of adsorbent: 15.0 mg; number of extraction cycles: 30 times; ionic strength: 5 %, NaCl; pH value: 7.0; elution solvent: 1.0 mL of ethanol: acetone (1:1).

Analytical performance

In order to investigate the practicality of the developed method, validation parameters including the linear ranges of calibration graphs, limits of detection (LODs), limits of quantification (LOQs), square of correlation coefficients (r^2), relative standard deviations (RSDs) and enrichment factors (EFs) were studied under optimized extraction conditions. The results obtained are summarized in Table 2. Linear ranges are between 1.0 and 100 ng mL^{-1} for all target analytes with square of correlation coefficients ranging from 0.9977 to 0.9990. Limits of detection (S/*N* = 3) and quantification (S/*N* = 10) were in the range of 0.3–0.6 and 1.0–2.0 ng mL^{-1}, respectively. The precision (in terms of RSD) of the method, calculated for six replicate measurements at concentration level 10.0 ng mL^{-1} of mixture PAHs, were in the range of 3.49 % to 5.94 %. The enrichment factors (EFs), defined as the ratio between the analyte concentration in the final extracted phase and the initial concentration of analytes, were in the range of 59.0 to 98.5.

Effect of foreign species

To test the applicability of this method in different matrix, the effects of the possible interfering foreign species on the simultaneous preconcentration and determination of PAHs were considered under the optimum conditions. The results showed

Table 2 Analytical figures of merit for the AA-dμ-SPE method

Analyte	LOD[a] (ng mL^{-1})	LOQ[b] (ng mL^{-1})	Linear range (ng mL^{-1})	Regression equation	r^2 [c]	RSD % (n = 6)	EF[d]
Naphthalene	0.6	2.0	1.0–100	y = 38.70× + 0.28	0.9977	3.68	68.2
Fluorene	0.5	1.7	1.0–100	y = 34.35× + 0.35	0.9981	3.49	59.0
Phenanthrene	0.4	1.3	1.0–100	y = 40.71× + 0.37	0.9983	4.37	69.2
Anthracene	0.5	1.7	1.0–100	y = 59.71× + 0.26	0.9990	4.18	98.5
Pyrene	0.3	1.0	1.0–100	y = 57.88× + 0.45	0.9988	5.94	93.4

[a] Limit of detection, S/N = 3

[b] Limit of quantification, S/N = 10

[c] Correlation coefficient

[d] Enrichment factor, EF = C_{ex}/C_0

that the presence of 1000-fold benzoic acid, salicylic acid, chlorophenols (including of 2-chlorophenol, 3-chlorophenol, 4-chlorophenol, 2,4,5-trichlorophenol) and 500-fold sedative drugs (including tramadol and acetaminophen) have no interference on the analytes recoveries (Table 1s).

Reusability of g-C_3N_4/Fe_3O_4

In this work, to investigate the recyclability of the adsorbent, g-C_3N_4/Fe_3O_4 was reused in AA-dμ-SPE method. After seven times of recycling, there was no obvious decrease or increase in the analytes relative response. Based on the obtained results, g-C_3N_4/Fe_3O_4 did not show any memory effects during successive extraction (up to seven times), indicating good reusability of this compound.

Comparison of the method with other works

This method was compared with other previous extraction methods that were used for the determination of PAHs in real

Table 3 Comparison of different methods for PAHs extraction

Method	adsorbent	Amount of adsorbent (mg)	Detection	Linear range (ng mL^{-1})	LODs (ng mL^{-1})	EF[a]	Extraction Time (min)	Refs.
μ-SPE[b]	ZIF-8[c]	-	GC-MS[d]	0.1–50	0.002–0.012	-	12	[2]
Dμ-SPE	nylon 6 composite	40.0	UPLC[e]-DAD[f]	-	0.050–0.580	18.1–43.5	32	[28]
μ-SPE	CTAB/TiO_2[g]	-	HPLC-UV[h]	0.2–100.0	0.026–0.82	-	≈66	[29]
μ-SPE	MWCNT[k]	30	GC-MS	0.1–50.0	0.0042–0.0465	132–138	30	[30]
SPE[l]	copolymer of pyrrole and phenol on steel frits	150	HPLC-UV	0.1–500	0.01–0.08	-	≈50	[3]
SPE	MWCNT	150	GC-MS	0.02–5.00	0.002–0.0085	-		[31]
MSPE[m]	carbon-ferromagnetic nanocomposite	10.0	GC-MS	0.5–80	0.015–0.335	35–133	45	[32]
MSPE	C_{18}/Fe_3O_4	50.0	GC-MS	10.0–800.0	0.8–36	-	≈6	[33]
MSPE	Fe_3O_4/GO[n]	40.0	HPLC-UV	0.5–100	0.09–0.19	-	10	[17]
AA-dμ-SPE	g-C_3N_4/Fe_3O_4	15.0	GC-FID	1.0–100	0.30–0.60	59–99	3	This work

[a] Enrichment factor

[b] Micro-solid phase extraction

[c] Zeolite imidazolate framework 8

[d] Gas chromatography–mass spectrometry

[e] Ultra performance liquid chromatography

[f] Diode array detect

[g] Cetyltrimethylammonium bromide modified TiO_2 nanotube arrays

[h] High-performance liquid chromatography–ultraviolet-visible

[k] Multiwall carbon nanotube

[l] solid phase extraction

[m] Magnetic solid phase extraction

[n] Graphene oxide

Table 4 Results for the determination of PAHs in saliva and blood sample

Analyte	Adedd (ng mL^{-1})	Saliva			Blood			Waste water		
		Found (ng mL^{-1})	RSD%	R%[a]	Found (ng mL^{-1})	RSD %	R%	Found (ng mL^{-1})	RSD %	R%
Naphthalene	0.0	6.87 ± 0.38	5.51	-	ND[b]	-	-	ND	-	-
	10.0	16.53 ± 0.59	3.57	97.98	9.60 ± 0.29	3.02	96.00	9.72 ± 0.37	3.81	97.20
	20.0	26.43 ± 1.02	3.86	98.36	19.41 ± 0.63	3.25	97.05	19.72 ± 0.73	3.70	98.60
Fluorene	0.0	8.93 ± 0.49	5.52	-	ND	-	-	ND	-	-
	10.0	18.35 ± 0.62	3.38	96.93	9.76 ± 0.36	3.69	97.60	9.81 ± 0.39	3.98	98.10
	20.0	28.23 ± 0.93	3.29	97.58	19.48 ± 0.66	3.39	97.40	19.67 ± 0.81	4.12	98.35
Phenanthrene	0.0	6.50 ± 0.40	6.15	-	ND	-	-	ND	-	-
	10.0	15.83 ± 0.58	3.66	95.93	9.55 ± 0.31	3.24	95.50	9.69 ± 0.34	3.51	96.90
	20.0	25.24 ± 0.85	3.37	95.24	19.36 ± 0.69	3.56	96.80	19.50 ± 0.60	3.08	97.5
Anthracene	0.0	3.13 ± 0.21	6.64	-	ND	-	-	ND	-	-
	10.0	12.67 ± 0.46	3.63	96.50	9.61 ± 0.36	3.75	96.10	9.81 ± 0.38	3.87	98.10
	20.0	21.96 ± 0.91	4.14	94.94	19.40 ± 0.78	4.02	97.00	19.32 ± 0.77	3.99	96.60
Pyrene	0.0	2.30 ± 0.15	6.52	-	ND	-	-	ND	-	-
	10.0	11.87 ± 0.73	6.15	96.50	9.57 ± 0.61	6.37	95.70	9.85 ± 0.54	5.64	98.50
	20.0	21.98 ± 1.32	6.01	98.57	19.67 ± 1.11	5.64	98.35	19.70 ± 0.98	4.97	98.50

[a] R, recovery

[b] ND, not detected

samples [2, 3, 17, 28–33]. Table 3 demonstrates the amount of adsorbent, linear range, limits of detection, enrichment factor, and extraction time of some analytical methods along with this work. As can be seen in Table 2, the present method requires a lower amount of adsorbent in comparison to most of other methods and lower extraction time (3 min) in comparison to

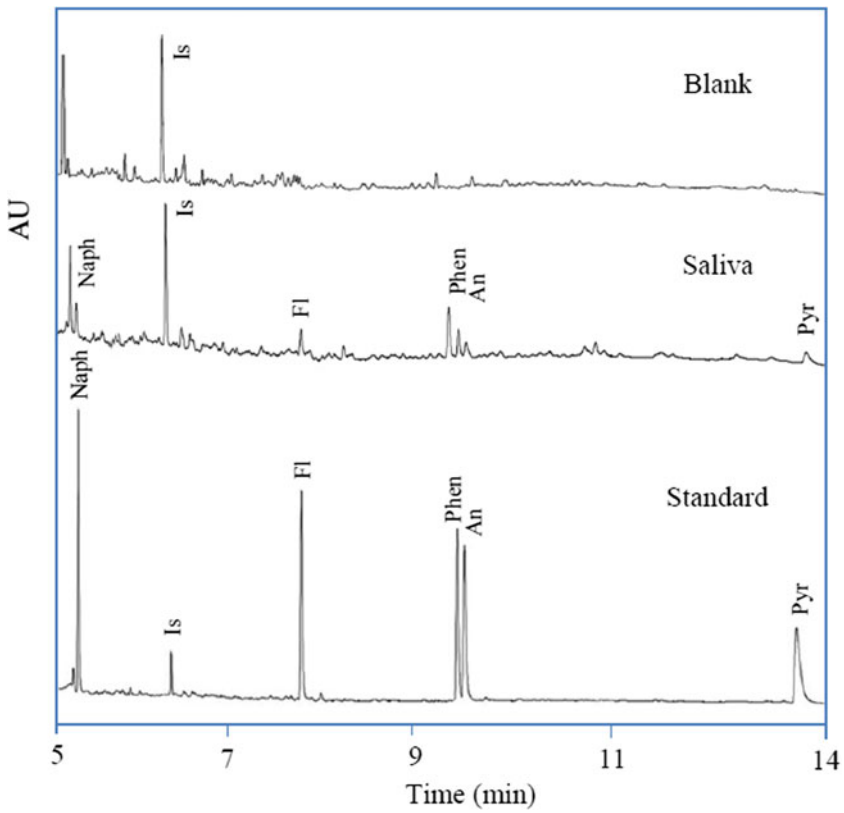

Fig. 4 GC-FID chromatograms of standard (with 10 μg mL^{-1} of each analyte), saliva and blank. In all cases, AA-dμ-SPE method was performed and 1 μL of the extraction phase was injected into GC

others. In general, linear range of method is wider than those of the mentioned methods. Hence, this method has several advantages over the other reported techniques, while it is also very simple, rapid and less hazardous for environment.

Real sample analysis

In the optimal conditions, the method was applied for determination of PAHs in the different real samples including saliva, blood and waste waters of Semnan city. The results are listed in Table 4. The recoveries of PAHs for spiked samples were in the range from 94.94 % to 98.60 %. None of the analytes were detected in blood and waste water. Target analytes was found in the saliva sample. The concentrations of naphthalene, fluorene, phenanthrene, anthracene and pyrene were calculated as 68.7 ± 3.8, 89.3 ± 4.9, 65.0 ± 4.0, 31.3 ± 2.1 and 23.0 ± 1.5 ng mL^{-1} (n = 3), respectively. The typical chromatograms for saliva samples are shown in Fig. 4.

Conclusion

In this study, air-assisted dispersive micro-solid phase extraction as a sample preparation method coupled to GC-FID was developed for the pre-concentration/determination of PAHs in waste water, saliva and blood samples. Different techniques including FTIR, XRD, TGA, SEM and TEM confirmed the successful synthesis and preparation of the adsorbent (g-C_3N_4/Fe_3O_4). The method is simple, efficient and environmental-friendly because a little amount of adsorbent was used, without using a toxic organic solvent as eluent. The main advantage of this method is simplicity of collection of g-C_3N_4/Fe_3O_4 nanocomposites based on magnetic properties, short extraction time in comparison to other methods. The results revealed that the developed method was suitable for determination of PAHs at ng mL^{-1} levels in complex matrices such as waste water, saliva and blood samples.

Acknowledgments The authors would like to thank Semnan University Research Council for the financial support of this work.

Compliance with Ethical Standards The author(s) declare that they have no competing interests

References

1. Leong MI, Chang CC, Fuh MR, Huang SD (2010) Low toxic dispersive liquid–liquid microextraction using halosolvents for extraction of polycyclic aromatic hydrocarbons in water samples. J Chromatogr A 1217: 5455–5461. doi:10.1016/j.chroma.2010.06.056
2. Ge D, Lee HK (2011) Water stability of zeolite imidazolate framework 8 and application to porous membrane-protected micro-solid-phase extraction of polycyclic aromatic hydrocarbons from environmental water samples. J. Chromatogr A 1218: 8490–8495. doi:10.1016/j.chroma.2011.09.077
3. Rahimi M, Noroozian E (2014) Application of copolymer coated frits for solid-phase extraction of poly cyclic aromatic hydrocarbons in water samples. Anal Chim Acta 836: 45–52. doi:10.1016/j.aca.2014.05.040
4. Barfi B, Asghari A, Rajabi M, Barfi A, Saeidi I (2013) Simplified miniaturized ultrasound-assisted matrix solid phase dispersion extraction and high performance liquid chromatographic determination of seven flavonoids in citrus fruit juice and human fluid samples: hesperetin and naringenin as biomarkers. J Chromatogr A 1311: 30–40. doi:10.1016/j.chroma.2013.08.078
5. Barfi B, Rajabi M, Morshedi Zadeh M, Ghaedi M, Niasari MS, Sahraei R (2015) Extraction of ultra-traces of lead, chromium and copper using ruthenium nanoparticles loaded on activated carbon and modified with N,N-bis-(α-methylsalicylidene)-2, 2-dimethylpropane-1,3-diamine. Microchim Acta 182: 1187–1196. doi:10.1007/s00604-014-1434-z
6. Rajabi M, Barfi B, Asghari A, Najafi F, Aran R (2015) Hybrid amine-functionalized titania/silica nanoparticles for solid-phase extraction of lead, copper, and zinc from food and Water samples: kinetics and equilibrium studies. Food Anal Methods 8:815–824. doi:10.1007/s12161-014-9964-x
7. Rajabi M, Esfandiari SH, Barfi B, Ghanbari H (2014) Ultrasound-assisted temperature-controlled ionic-liquid dispersive liquid-phase microextraction method for simultaneous determination of anethole, estragole, and para-anisaldehyde in different plant extracts and human urine: a comparative study. Anal Bioanal Chem 406: 4501–4512. doi:10.1007/s00216-014-7848-y
8. Rajabi M, Ghanbari H, Barfi B, Asghari A, Esfandiari SH (2014) Ionic liquid-based ultrasound-assisted surfactant-emulsified microextraction for simultaneous determination of three important flavoring compounds in plant extracts and urine samples. Food Res Int 62: 761–770. doi:10.1016/j.foodres.2014.04.034
9. Mirnaghi FS, Monton MRN, Pawliszy J (2012) Thin-film octadecyl-silica glass coating for automated 96-blade solid-phase microextraction coupled with liquid chromatography–tandem mass spectrometry for analysis of benzodiazepines. J Chromatogr A 1246: 2–8. doi:10.1016/j.chroma.2011.11.030
10. Kaykhaii M, Dicinoski GW, Smedley R, Pawliszyn J, Haddad PR (2010) Preparation and evaluation of solid-phase microextraction fibres based on functionalized latex nanoparticle coatings for trace analysis of inorganic anions. J Chromatogr A 1217: 3452–3456. doi:10.1016/j.chroma.2010.03.047
11. Fard VK, Ghanemi K, Nikpour Y, Mehrjardi MF (2012) Application of sulfur microparticles for solid-phase extraction of polycyclic aromatic hydrocarbons from sea water and wastewater samples. Anal Chim Acta 714: 89–97. doi:10.1016/j.aca.2011.11.065
12. Song X, Li J, Xu JLS, Ying R, Ma J, Liao C, Liu D, Yu J, Chen L (2012) Determination of 16 polycyclic aromatic hydrocarbons in seawater using molecularly imprinted solid-phase extraction coupled with gas chromatography-mass spectrometry. Talanta 99: 75–82. doi:10.1016/j.talanta.2012.04.065
13. Pourreza N, Ghanemi K (2009) Determination of mercury in water and fish samples by cold vapor atomic absorption spectrometry after solid phase extraction on agar modified with 2-mercaptobenzimidazole. J Hazard Mater 161: 982–987. doi:10.1016/j.jhazmat.2008.04.043
14. Luo X, Zhang F, Ji S, Yang B, Liang X (2014) Graphene nanoplatelets as a highly efficient solid-phase extraction sorbent for determination of phthalate esters in aqueous solution. Talanta 120: 71–75. doi:10.1016/j.talanta.2013.11.079
15. Shen Q, Gong L, Baibado JT, Dong W, Wang Y, Dai Z, Cheung HY (2013) Graphene based pipette tip solid phase extraction of marine

toxins in shellfish muscle followed by UPLC–MS/MS analysis. Talanta 116: 770–775. doi:10.1016/j.talanta.2013.07.042
16. Mahpishanian S, Sereshti H (2014) Graphene oxide-based dispersive micro-solid phase extraction for separation and preconcentration of nicotine from biological and environmental water samples followed by gas chromatography-flame ionization detection. Talanta 130: 71–77. doi:10.1016/j.talanta.2014.06.004
17. Han Q, Wang Z, Xia J, Chen S, Zhang X, Ding M (2012) Facile and tunable fabrication of Fe_3O_4/graphene oxide nanocomposites and their application in the magnetic solid phase extraction of polycyclic aromatic hydrocarbons from environmental water samples. Talanta 101: 388–395. doi:10.1016/j.talanta.2012.09.046
18. Shalom M, Inal S, Fettkenhauer C, Neher D, Antonietti M)2013) Improving Carbon Nitride Photocatalysis by Supramolecular Preorganization of Monomers. J Am Chem Soc 135: 7118–7121. doi:10.1021/ja402521s
19. Portehault D, Giordano C, Gervais C, Senkovska I, Kaskel S, Sanchez C, Antonietti M (2010) High-surface-area nanoporous boron carbon nitrides for hydrogen storage. Adv Funct Mater 20: 1827–1833. doi:10.1002/adfm.201000281
20. Wu M, Wang Q, Sun Q, Jena P (2013) Functionalized graphitic carbon nitride for efficient energy storage. J Phys Chem C 117: 6055–6059. doi:10.1021/jp311972f
21. Cheng C, Huang Y, Wang J, Zheng B, Yuan H, Xiao D (2013) Anodic electrogenerated chemiluminescence behavior of graphite-like carbon nitride and its sensing for rutin. Anal Chem 85 2601–2605. doi:10.1021/ac303263n
22. He J, Huang M, Wang D, Zhang Z, Li G (2014) Magnetic separation techniques in sample preparation for biological analysis. J Pharm Biomed Anal 101: 84–101. doi:10.1016/j.jpba.2014.04.017
23. Toh PY, Yeap SP, Kong LP, Ng BW, Chan DJC, Ahmad AL, Lim JK (2012) Magnetophoretic removal of microalgae from fishpond water: feasibility of high gradient and low gradient magnetic separation. Chem Eng J 211-212: 22–30. doi:10.1016/j.cej.2012.09.051
24. Barfi B, Asghari A, Rajabi M, Sabzalian S, Khanalipoor F, Behzad M (2015) Optimized syringe-assisted dispersive micro solid phase extraction coupled with microsampling flame atomic absorption spectrometry for the simple and fast determination of potentially toxic metals in fruit juice and bio-fluid samples, RSC Advances 5: 31930–31941. doi:10.1039/C5RA03537F
25. Xu N, Wang Y, Rong M, Ye Z, Deng Z, Chen X (2014) Facile preparation and applications of graphitic carbon nitride coatingin solid-phase microextraction. J Chromatogr A 1364: 53–58. doi:10.1016/j.chroma.2014.08.081
26. Kumar S, Surendar T, Kumar B, Baruah A, Shanker V (2013) Synthesis of magnetically separable and recyclable g-C_3N_4 − Fe_3O_4 hybrid nanocomposites with enhanced photocatalytic performance under visible-light irradiation. J Phys Chem C 117: 26135–26143. doi:10.1021/jp409651g
27. Katsumata KI, Motoyoshi R, Matsushita N, Okada K (2013) Preparation of graphitic carbon nitride (g-C_3N_4)/WO_3 composites and enhanced visible-light-driven photodegradation of acetaldehyde gas. J Hazard Mater 260: 475–482. doi:10.1016/j.jhazmat.2013.05.058
28. Gallardo EMR, Lucena R, Cárdenas S, Valcárcel M (2014) Magnetic nanoparticles-nylon 6 composite for the dispersive microsolid phase extraction of selected polycyclic aromatic hydrocarbonsfrom water samples. J Chromatogr A 1345: 43–49. doi:10.1016/j.chroma.2014.04.033
29. Huang Y, Zhou Q, Xie G (2011) Development of micro-solid phase extraction with titanate nanotube array modified by cetyltrimethylammonium bromide for sensitive determination of polycyclic aromatic hydrocarbons from environmental water samples. J Hazard Mater 193: 82–89. doi:10.1016/j.jhazmat.2011.07.025
30. Guo L, Lee HK (2011) Development of multiwalled carbon nanotubes based micro-solid-phase extraction for the determination of trace levels of sixteen polycyclic aromatic hydrocarbons in environmental water samples. J Chromatogr A 1218: 9321–9327. doi:10.1016/j.chroma.2011.10.066
31. Ma J, Xiao R, Li J, Yu J, Zhang Y, Chen L (2010) Determination of 16 polycyclic aromatic hydrocarbons in environmental water samples by solid-phase extraction using multi-walled carbon nanotubes as adsorbent coupled with gas chromatography–mass spectrometry. J Chromatogr A 1217: 5462–5469. doi:10.1016/j.chroma.2010.06.060
32. Bai L, Mei B, Guo QZ, Shi ZG, Feng YQ (2010) Magnetic solid-phase extraction of hydrophobic analytes in environmental samples by a surface hydrophilic carbon-ferromagnetic nanocomposite. J Chromatogr A 1217: 7331–7336. doi:10.1016/j.chroma.2010.09.060
33. Liu Y, Li HF, Lin JM (2009) Magnetic solid-phase extraction based on octadecyl functionalization of monodisperse magnetic ferrite microspheres for the determination of polycyclic aromatic hydrocarbons in aqueous samples coupled with gas chromatography–mass spectrometry. Talanta 77: 1037–1042. doi:10.1016/j.talanta.2008.08.013